Volume 385, issue 2 15 November 2007 ISSN 0378-4371

Available online at
ScienceDirect
www.sciencedirect.com
http://www.elsevier.com/locate/physa

Available online at www.sciencedirect.com
ScienceDirect
Physica A 385 (2007) 527–542
PHYSICA A
www.elsevier.com/locate/physa

Cluster formation in mesoscopic systems

Elena Kartashova*, Guenther Mayrhofer

RISC, J. Kepler University, Linz 4040, Austria

Received 22 March 2007; received in revised form 17 May 2007
Available online 26 July 2007

Abstract

Graph-theoretical approach is used to study cluster formation in mesocsopic systems. Appearance of these clusters is due to discrete resonances which are presented in the form of a multigraph with labeled edges. This presentation allows to construct all non-isomorphic clusters in a finite spectral domain and generate corresponding dynamical systems automatically. Results of MATHEMATICA implementation are given and two possible mechanisms of cluster destroying are discussed.

PACS: 47.27.E−; 67.40.Vs; 67.57.Fg

Keywords: Mesoscopic systems; Discrete resonances; Graph-theoretical approach; Dynamics

1. Introduction

Mesoscopic regimes are at the frontier between classical (single waves/particles) and statistical (infinite number of waves/particles) description of physical systems. Mesoscopic systems is a very popular topic in various areas of modern physics and can be met in wave turbulence theory, condensed matter (quantum dots), sociology (opinion formation), medicine (dynamics of cardiovascular system), etc. For instance, statistical wave turbulence theory is based on Kolmogorov's suggestion about spatial evenness of turbulence and does not describe observed organized structures extending over many scales like boulders in a waterfall. Also many laboratory experiments stay unexplained in terms of statistical approach as in Ref. [1] where the experimental results have been presented for water turbulence excited by piston-like programmed wave-makers in water flume with dimensions $6 \times 12 \times 1.5$ m. The main goal of this experiments was to establish a power-law scaling for the energy spectrum, $E \sim \omega^{-\nu}$, with some fixed ν coming from statistical considerations and ω being wave dispersion function. It turned out that discrete effects are major and statistical predictions are never achieved: with increasing wave intensity the nonlinearity becomes strong before the system loses sensitivity to the discreteness of the spectral space.

*Corresponding author. Tel.: +43 732 918383; fax: +43 732 2468 9930.
E-mail addresses: elena.kart@gmx.at, lena@risc.uni-linz.ac.at (E. Kartashova), guenther.mayrhofer@risc.uni-linz.ac.at (G. Mayrhofer).

0378-4371/$ - see front matter © 2007 Elsevier B.V. All rights reserved.
doi:10.1016/j.physa.2007.07.035

Our next example is taken from a quite different area of research—sociology. Finite-size effects in the dynamics of opinion formation have been profoundly studied quite recently in Ref. [2] with essentially the same conclusions made. Namely, some changes of a system can be observed only when "finite number of agents in the model takes a finite value" and thermodynamic limit does not describe behavior of these systems. It was shown that resonance by which a finite-size system is optimally amplified by a weak forcing signal (identified as an advertising agent) is determined by *the size* of mesoscopic system and the largest peak of the spectral density is observed at the driving frequency.

Another interesting example of a mesoscopic system can be found in Ref. [3] where the flow of blood through the system of closed tubes—the blood vessels—is described by wave equations. A model of the cardiovascular system as a system of coupled oscillators is proposed and conditions of their resonance are studied.

Now the question is: what have boulders in waterfalls, advertisement and cardiovascular system in common? From mathematical point of view the answer is very simple: dynamics of all these systems can be interpreted as *discrete* resonances. Notice that resonance conditions have the same general form for wave and quantum systems (see, for instance [4] for 4-photon processes) and have to be studied in integers. In this paper we have chosen a wave turbulent system as our main example and therefore use wave terminology.

From now on we regard resonance conditions of the form

$$\omega_1 \pm \omega_2 \pm \cdots \pm \omega_s = 0, \quad \vec{k}_1 \pm \vec{k}_2 \pm \cdots \pm \vec{k}_s = 0, \tag{1}$$

where $\omega_i = \omega(\vec{k}_i)$, $s < \infty$, with $\vec{k}$ and $\omega_i = \omega(\vec{k}_i)$ being correspondingly wave vector and dispersion function. Specific features of these systems described by Fourier harmonics with integer mode numbers were first studied in Ref. [5] (we call them further discrete wave systems, DWS). It is well-known that fully statistical description of a wave turbulent system yields wave kinetic equation [6] analogous to kinetic equation known in quantum mechanics. A counter part to kinetic equation in DWS is a set of few *independent* dynamical systems of ODEs on the amplitudes of interacting waves. The theory presented in Ref. [5] was based on a collection of pure existence theorems [7] and has been developed with the understanding that discrete effects are only important for small $|\vec{k}|$ of order ~ 10 while in larger spectral domains statistical regimes do occur. Numerous results of the last few years ([8–14] just to mention a few of them) showed that the general conception—discrete effects are only important in small spectral domains—should be revised because these effects are in fact observed in systems where thousands of Fourier harmonics are taken into account, i.e. in a wide range of mesoscopic wave systems. A model of laminated wave turbulence has been presented in Ref. [15] which explains the appearance of coherent structures in arbitrarily big but finite spectral domains. This model put forward a novel computational problem of solving (1) in integers of the order of 10^3 and more. Fast generic algorithms for a big class of irrational and rational dispersion functions have been developed in Ref. [16] which can be used for a wide range of dispersion functions; they were also implemented (for cases $s = 3$ and 4) and computation time on a Pentium-3 is of order 5–15 min in computation domain $|m|, |n| \leqslant 10^3$, where $\vec{k} = (m, n)$, $m, n \in \mathbb{Z}$. Straightforward computations for the same examples (without using our algorithms) take few days with a similar computer and computation domains of the order of 10^2.

It is important to realize that the notion of "small" and "big" wave numbers depends drastically on the physical system under consideration. For instance, when climate variability is studied in the frame of the barotropic vorticity equation (BVE) on a sphere, planetary waves are regarded with lengths comparable to the radius of the Earth, and this yields $|m|, |n|$ of the order of 20–30. The study of the ocean planetary waves leads to the spectral domains of the order of 100–200 while investigation of gravity water waves is normally performed in the spectral domains of the order of 10^3, and the problems of superconductivity might lead to substantially larger spectral domains. Knowing the wave lengths, a researcher can easily transform the covering dimensioned equation into its normalized non-dimensioned form and find out the corresponding spectral domain.

In this paper we study the structure of the solution set of (1) using graph-theoretical approach and develop a special technique to construct all independent clusters and corresponding dynamical systems. We present the whole solution set as a multigraph with labeled edges so that each connected component of this multigraph correspond to a special dynamical system of ODEs on the wave amplitudes. The most important fact about is this construction is the following: it provides simultaneous isomorphism of multigraph components and

dynamical systems. Using algorithms [16] we have developed a MATHEMATICA program package (at present only for $s = 3$ and 2D-waves) capable to (1) construct all independent clusters of the solution set of (1) in a given computation domain; (2) draw them as a multigraph on a plane; (3) write out explicitly all dynamical systems appearing in a chosen spectral domain. Some results of our implementation are given, possible directions for further research are briefly discussed.

2. Discrete 3-wave resonances

As our main example, 3-wave resonances covered by BVE [17] has been chosen. This equation, also known as Obukhov–Charney or Hasegawa–Mima equation, is important in many physical applications—from geophysics to astrophysics to plasma physics: the equation was again and again re-discovered by specialists in very different branches of physics. In particular, this equation describes ocean planetary waves

$$\frac{\partial \Delta\psi}{\partial t} + \beta \frac{\partial \psi}{\partial x} = -\varepsilon J(\psi, \Delta\psi) \tag{2}$$

with non-flow boundary conditions in a rectangular domain

$$\psi = 0 \text{ for } x \in [0, L_x], \quad y \in [0, L_y],$$

where β is a constant called Rossby number, $0 < \varepsilon \ll 1$ is a small parameter and Jacobean has the standard form

$$J(a, b) = \frac{\partial a}{\partial x}\frac{\partial b}{\partial y} - \frac{\partial a}{\partial y}\frac{\partial b}{\partial x}.$$

A linear wave has then the form [18]

$$A \cos\left(\frac{\beta}{2\omega}x + \omega t\right) \sin\frac{\pi m}{L_x}x \sin\frac{\pi n}{L_y}y, \qquad m, n \in \mathbb{Z}$$

and dispersion function can be written as

$$\omega = 2/\beta \sqrt{\left(\frac{\pi m}{L_x}\right)^2 + \left(\frac{\pi n}{L_y}\right)^2}.$$

After obvious re-normalization we write out resonance conditions for 3-wave interactions as follows:

$$\begin{cases} \dfrac{1}{\sqrt{m_1^2 + n_1^2}} \pm \dfrac{1}{\sqrt{m_2^2 + n_2^2}} = \dfrac{1}{\sqrt{m_3^2 + n_3^2}} \\ n_1 \pm n_2 = n_3. \end{cases} \tag{3}$$

This system will be our main subject of study in this paper.

Just for completeness of presentation we present here a simple idea underlying our algorithm for computing integer solutions of (3) (for more details see Ref. [16]). It was noticed that (3) has integer solutions only if all three numbers $\sqrt{m_i^2 + n_i^2}$, $i = 1, 2, 3$, have the same irrationality, i.e. can be presented as

$$\sqrt{m_i^2 + n_i^2} = \gamma_i \sqrt{q} \tag{4}$$

with some integer γ_i called *weight* and the same square-free q called *index*. In this way, the set of all wave vectors can be divided into non-intersecting classes Cl_q according to class index and solutions are to be looked for in each class separately. It is important to realize that this is only a necessary condition for a solution to exist and some classes can be empty.

As a first step, we compute the set of all possible indexes q. Due to the Lagrange theorem on presentation of an integer as a sum of two squares we conclude that q should not be divisible by any prime of the form $p = 4u + 3$ which reduces the full search substantially. Special algorithms for representing square-free numbers as sums of two squares are known, and one of them [19] was used in numerical implementation of our algorithm to compute the set of all possible numbers $q\gamma_i^2$ such that all g_i satisfy weight equation (5). Special

number-theoretical considerations allowed us to disregard a lot of classes from computations (about 74% of all classes in the domain $m, n \leqslant 1000$) as being empty.

Next we have to find integer solutions of the weight equation

$$\frac{1}{\gamma_1} + \frac{1}{\gamma_2} = \frac{1}{\gamma_3}. \tag{5}$$

At this step the number of variables is reduced from 6 to 3 and of their individual degrees from 2 to 1, and we got rid from irrationality in (5). Solutions are looked for only for indexes found at the previous step. At this step all solutions of the first equation of (3) are already found. Finally, we check linear conditions on n_i, that is, we check whether the second equation of (3) is fulfilled.

In the MATHEMATICA implementation, standard functions for list operations and some number-theoretical function, like `SquareFreeQ` and `SumOfSquaresRepresentations`, from the standard package "NumberTheoryFunctions" are used (for details see Ref. [20]).

3. Naive graph presentation

The graphical way to present 2D-wave resonances suggested in Ref. [7] for 3-wave interactions is to regard each 2D-vector as a node of integer lattice in the spectral space and connect those nodes which construct one solution (triad, quartet, etc.) We demonstrate the result in Fig. 1 in the upper panel. Obviously, the geometrical structure is too nebulous to be useful even in relatively small spectral domains. On the other hand,

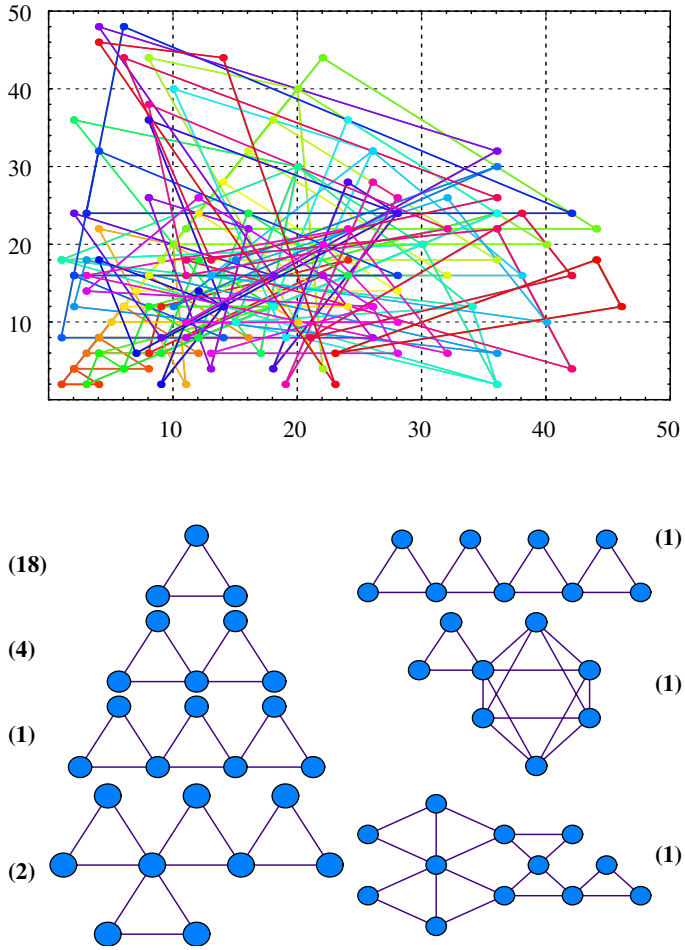

Fig. 1. **Upper panel:** Example of geometrical structure, spectral domain $|k_i| \leqslant 50$. **Lower panel:** Example of topological structure, the same spectral domain. The number in brackets shows how many times corresponding cluster appears in the chosen spectral domain.

topological structure shown in Fig. 1 (lower panel) is quite clear and gives us immediate information about dynamical equations covering behavior of each wave cluster.

Indeed, energy transport is covered by a standard dynamical system, written for simplicity for real-valued amplitudes,

$$\dot{A}_1 = \alpha_1 A_2 A_3, \quad \dot{A}_2 = \alpha_2 A_1 A_3, \quad \dot{A}_3 = \alpha_3 A_1 A_2 \tag{6}$$

in case of a "triangle" group called further *a primary element*: (A_1, A_2, A_3); by

$$\dot{A}_1 = \alpha_1 A_2 A_3, \quad \dot{A}_2 = \alpha_2 A_1 A_3, \quad \dot{A}_3 = \tfrac{1}{2}(\alpha_3 A_1 A_2 + \alpha_4 A_5 A_6), \quad \dot{A}_5 = \alpha_5 A_3 A_6, \quad \dot{A}_6 = \alpha_6 A_3 A_5 \tag{7}$$

in the case of a "butterfly" group (two connected triangle groups): $(A_1, A_2, A_3)(A_3, A_5, A_6)$, and so on. All isomorphic graphs presented in Fig. 1 are covered by similar dynamical systems, only magnitudes of interaction coefficients α_i vary. However, in the general case graph structure thus defined does not present the dynamical system unambiguously. Consider Fig. 2 where two objects are isomorphic *as graphs*. However, the first object represents four connected primary elements with dynamical system

$$(A_1, A_2, A_3), \quad (A_1, A_2, A_5), \quad (A_1, A_3, A_4), \quad (A_2, A_3, A_6) \tag{8}$$

while the second—three connected primary elements with dynamical system

$$(A_1, A_2, A_5), \quad (A_1, A_3, A_4), \quad (A_2, A_3, A_6). \tag{9}$$

To discern between these two cases we set a placeholder inside the triangle not representing a resonance, we call it further an empty *3-cycle*. This means that to determine isomorphism of dynamical systems we have to regard graph G together with some parameter(s) ξ to identify corresponding dynamical system uniquely. We call a pair (G, ξ) an *i-pair* if it provides isomorphism of dynamical systems. The set of possible parameters ξ (not exhaustive, of course) is: number of vertices, their multiplicities, number of edges, their multiplicities, number of primary elements (non-empty 3-cycles) N, the list of non-empty 3-cycles L_c, etc. Some preliminary study of the parameter set show that L_c and N is a good first choice, providing a balance between informativeness and complexity of numerical implementation.

Consider a structure (G_t, L_c) consisting of:

- a graph G_t each edge of which belongs to at least one 3-cycle;
- non-empty list L_c of some 3-cycles of length 3 of G_t such that each edge of G_t belongs to some cycle(s) of L_c.

Notice that L_c does not contain "wrong" triangles. Notation G_t has been chosen in order to point out that our graphs are, so to say, "triangle" graphs.

Definition 1. The number of elements in L_c is called the *order* of G_t and denoted as $N(G_t)$. Three-cycles of G_t *not* belonging to L_c are called *empty cycles*. The number of occurrences of each vertex $v \in G_t$ in L_c is called *vertex multiplicity* and denoted as $\mu(v)$. Number of different vertices in L_c is denoted as $M(G_t)$.

Obviously, G_t-graphs consisting of 3-cycles only have a very special structure. Our idea is to construct a set of all possible graphs of this type of order $\leqslant N$ for some given N inductively, beginning with a single triangle. As the next step we can choose all unisomorphic graphs from this set and compare the corresponding lists L_c to find all different dynamical systems.

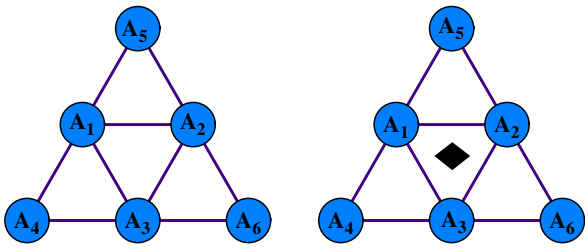

Fig. 2. Example of isomorphic graphs and unisomorphic dynamical systems. The left graph corresponds to the dynamical system (8) and the graph on the right—to the dynamical system (9).

3.1. Triangle gluing

The possibilities of gluing a new triangle to a G_t-graph are not numerous and can be classified as follows. Let the new Nth triangle be $T = \{v_1, v_2, v_3\}$.

- Vertex gluing. In this case, 1, 2 or 3 vertices of the new triangle are identified with (glued to) vertices of some *distinct triangles* of the graph, constructed at previous inductive step, $G_t^{(N_1)}$.
- Edge gluing. In this case, 1, 2 or 3 edges and corresponding vertices of the new triangle glued to edges and vertices of some *distinct adjacent triangles* of the graph. Notice that gluing of three edges is simply filling an empty triangle of $G_t^{(N-1)}$.
- Mixed gluing. In this case, one vertex v_{N_1} of the new triangle is glued to a vertex of some triangle of the graph and the edge $v_{N_2}v_{N_3}$ is glued to an edge of another triangle.

The cases described above are illustrated by Figs. 3–5.

- By vertex gluing, the $G_t^{(N-1)}$ structure is enhanced by:
  - two vertices and three edges (one vertex glued);
  - one vertex and three edges (two vertices glued);
  - three edges (three vertices glued).
- By edge gluing, the $G_t^{(N-1)}$ structure is enhanced by:
  - one vertex and two edges (one edge glued);
  - one edge (two edges glued);
  - the graph structure stays unchanged (three edges glued)
- By mixed gluing, the $G_t^{(N-1)}$ structure is enhanced by two edges.

In each case, the list $L_c^{(N-1)}$ of graph $G_t^{(N-1)}$ is extended by the $v_{N_1}v_{N_2}v_{N_3}$ cycle of the new triangle (or whatever these vertices will be called after the gluing).

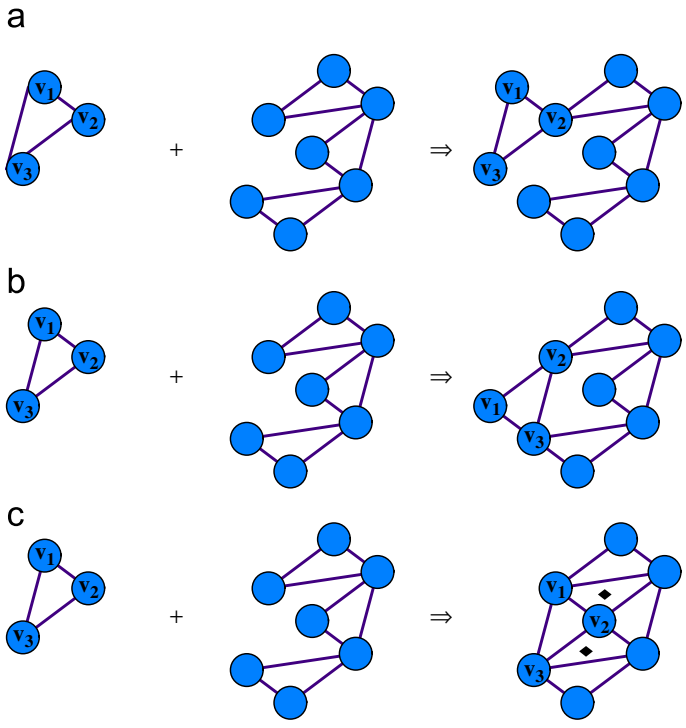

Fig. 3. Vertex gluing of a new triangle to $G_t^{(N-1)}$. (a) Gluing by one vertex. (b) Gluing by two vertices. (c) Gluing by three vertices.

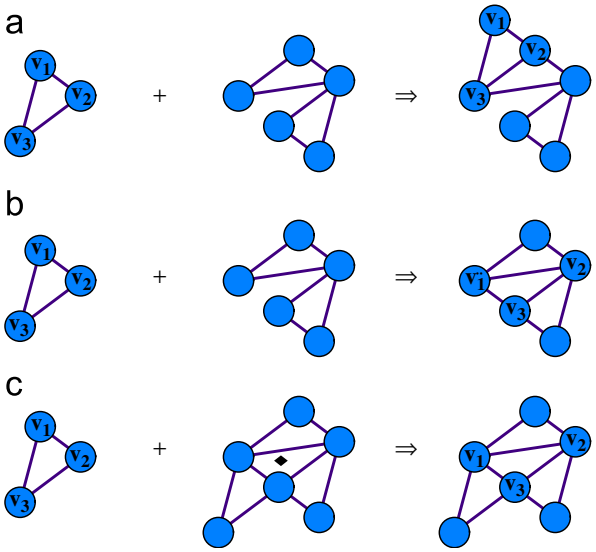

Fig. 4. Edge gluing of a new triangle to $G_t^{(N-1)}$. (a) Gluing by one edge. (b) Gluing by two edges. (c) Gluing by three edges.

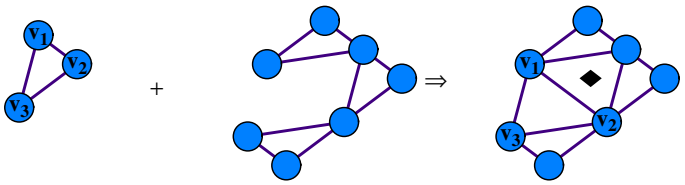

Fig. 5. Mixed gluing of a new triangle to $G_t^{(N-1)}$.

3.2. Some estimations

Enhancing a given G_t with V vertices and E edges by a triangle, we encounter the following possibilities:

- a sole triangle not connected to the existing graph is added (1 possibility);
- vertex gluing (V possibilities);
- edge gluing (E possibilities);
- mixed gluing—approximately $E/V(E/V-1)$ possibilities;
- filling an empty triangle (very rare).

Therefore at each inductive step the mean number of vertices is $V \leqslant 1.5N$ and the number of arcs can be roughly estimated as $E \leqslant 2N$. Therefore, the number of emerging unisomorphic graphs can be estimated from above as some $\sim 4N$ and the overall number of graphs at step N is $\mathcal{O}(N^2)$.

4. Hypergraph presentation

To diminish computational time and complexity we construct a *hypergraph* presentation of i-pairs introduced in the previous section. A hypergraph is a structure that consists of a set of vertices and a multiset of edges, called hyperedges. A hyperedge is a set of vertices, all vertices in such a set are connected. The collection of hyperedges is a multiset because it is possible that some hyperedges appear more times than once. A traditional graph is a special case of a hypergraph, in which all edges are two-element sets and do not appear more than once. For the representation of 3-wave resonances we consider the triangles as "the nodes" of the corresponding hypergraph.

Definition 2. A hypergraph with 3-cycles of a triangle graph G_t as its *vertices* and nodes (m, n) of G_t as its *edges* is called *a triangle hypergraph* and is denoted as HG_t. The sets of its vertices and edges are denoted as V_{HG} and E_{HG} correspondingly, i.e. $HG_t = (V_{HG}, E_{HG})$.

Notice that since a node $(\tilde{m}, \tilde{n})$ of G_t can belong to several 3-cycles, the corresponding HG_t has in fact hyperedges instead of edges of a simple graph. A hypergraph HG_t generated by G_t has two properties:

- Each vertex is a part of exactly three hyperedges.
- Each pair of vertices is a part of at most two hyperedges.

The first property follows from the fact, that each vertex of HG_t represents a 3-cycle which consists of three different nodes of G_t. If the second property is violated then the two associated 3-cycles of G_t have three nodes in common, hence they are identical.

As an illustrative example, let us write out explicitly a hypergraph presentation of the dynamical systems (8) and (9) presented in Fig. 2 at the left and right panel correspondingly:

$$(V_{HG} = \{1, 2, 3, 4\}, \quad E_{HG} = \{\{2\}, \{3\}, \{4\}, \{1, 2, 3\}, \{1, 2, 4\}, \{1, 3, 4\}\}) \tag{10}$$

and

$$(V_{HG} = \{1, 2, 3\}, \quad E_{HG} = \{\{1\}, \{2\}, \{3\}, \{1, 2\}, \{1, 3\}, \{2, 3\}\}). \tag{11}$$

4.1. Incidence matrix

For computation purposes it is convenient to represent a hypergraph HG_t by its incidence matrix which is constructed in the following way.

Definition 3. A rectangular matrix $\mathfrak{F} = (f_{i,j})$ with $M(G_t)$ columns and $N(G_t)$ rows is called the *incidence matrix of* G_t if

$$f_{i,j} = \begin{cases} 1 & j\text{th non-empty 3-cycle contains } i\text{th node}, \\ 0 & \text{otherwise}. \end{cases} \tag{12}$$

Each column of the matrix $\mathfrak{F}$ represents a triangle in the solution set of (3) while each row represents a node (see Definition 1). Since we are not interested in nodes themselves but in their relation to each other we can relabel the nodes of the triangle with ascending integers in an arbitrary way and use the labels of the nodes for indexing elements in a matrix. Now we can construct the hyperedges of HG_t: if the jth entry of a row is equal to 1 then we add j to this hyperedge. The vertices of HG_t are elements of L_c. The ordering of the hyperedges is not important, because it is a multiset. However, it is better to have a "normal form", so we sort the hyperedges by using some ordering. Since we are interested in an implementation in MATHEMATICA we choose the ordering used by the command `Sort`. This is an ordering, which orders lists ascending by their length, and lists of same length lexicographical by their elements. For dynamical systems there is no ordering with practical advantages for the implementation, so we let them unsorted. The incidence matrices of the dynamical systems (8) and (9) have the form

$$\begin{pmatrix} 1 & 1 & 1 & 0 \\ 1 & 1 & 0 & 1 \\ 1 & 0 & 1 & 1 \\ 0 & 0 & 1 & 0 \\ 0 & 1 & 0 & 0 \\ 0 & 0 & 0 & 1 \end{pmatrix} \tag{13}$$

and

$$\begin{pmatrix} 1 & 1 & 0 \\ 1 & 0 & 1 \\ 0 & 1 & 1 \\ 0 & 1 & 0 \\ 1 & 0 & 0 \\ 0 & 0 & 1 \end{pmatrix} \tag{14}$$

correspondingly. Analogously, incidence matrices of their hypergraphs, here we use the ordering of the hyperedges described above

$$\begin{pmatrix} 0 & 1 & 0 & 0 \\ 0 & 0 & 1 & 0 \\ 0 & 0 & 0 & 1 \\ 1 & 1 & 1 & 0 \\ 1 & 1 & 0 & 1 \\ 1 & 0 & 1 & 1 \end{pmatrix} \tag{15}$$

and

$$\begin{pmatrix} 1 & 0 & 0 \\ 0 & 1 & 0 \\ 0 & 0 & 1 \\ 1 & 1 & 0 \\ 1 & 0 & 1 \\ 0 & 1 & 1 \end{pmatrix} \tag{16}$$

are also different. The incidence matrices of a dynamical system and the corresponding hypergraph are not identical. The reason is the use of different orderings for the vertices. Matrix (15) is just a permuted version of matrix (13). Since we use a special ordering for the hyperedges, which are described by the rows of the incidence matrix, we obtain permuted rows. For identifying isomorphic dynamical systems it is not necessary to preserve an ordering, because dynamical systems with permuted elements are still isomorphic. Hence, neither row permutations nor column permutations destroy the isomorphism of dynamical systems. In this example only row permutations occur, permutations of columns are just another ordering of the elements of L_c. This construction can be redone and the dynamical system can be reconstructed from its hypergraph: by considering the columns of this matrix we know which nodes belong to a certain 3-cycle.

Obviously, if two hypergraphs (10) and (11) are not isomorphic, their incidence matrices (13) and (14) are also different. But in general for the final decision it is necessary to have an algorithm to establish isomorphism of hypergraphs. Since there are not so many general algorithms for hypergraphs one has to find a representation where it would be possible to use standard algorithms for graph isomorphism. This leads us to auxiliary multigraph construction presented in the next section.

4.2. Multigraph construction

A multigraph MG_t is constructed in the following way. Its vertices coincide with the vertices of HG_t and each hyperedge is replaced by all the two-element subsets. To maintain the whole information we have to label the created edges so that edges which belong to the same hyperedge of HG_t are labeled identically. These labels allow to reconstruct HG_t and $\mathfrak{F}$ which is a necessary step while generating dynamical systems. The hyperedges which contain only one vertex can be omitted because they contain no further information about the cluster structure.

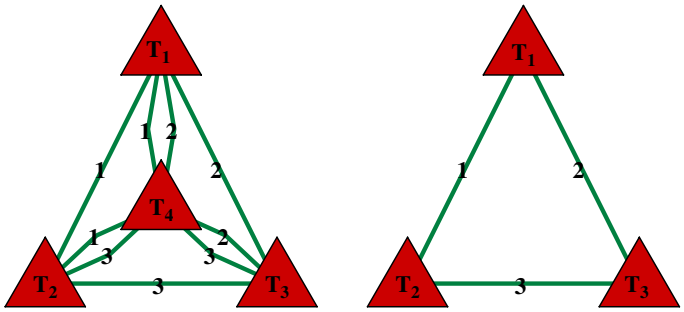

Fig. 6. The left multigraph corresponds to the dynamical system (8) and the multigraph on the right—to the dynamical system (9).

Of course, some edges may occur in MG_t twice—this is the case if two 3-cycles of G_t share two nodes. Fig. 6 shows two multigraphs corresponding to the dynamical systems shown in Fig. 2. For easier distinction weuse triangle symbols for the vertices of the multigraphs, because a vertex represents a 3-cycle of G_t.

A multigraph MG_t has the following properties:

- At most two edges connect a pair of vertices.
  It follows from the fact that a pair of 3-cycles can share at most two nodes. If they would share also their third node, they would be identical.
- At most three differently labeled edges can occur at a vertex.
  A 3-cycle has three nodes therefore it can only share three different nodes with other 3-cycles.
- The number of vertices is equal to the number of non-empty 3-cycles in G_t.
  By definition.
- The total number of edges with identical labels is $(p-1)p/2$, where p is the number of elements in the corresponding hyperedge.
  Edges with identical labels belong to the same hyperedge, and the number of two-element subsets is $\binom{p}{2}$.

4.3. Hypergraph versus naive graph

Summarizing briefly the procedure described above, the following has been done:

- all integer solutions of (3) have been found;
- topological presentation of the solution set as an i-pair (G_t, L_c) has been constructed which presents corresponding dynamical system uniquely up to isomorphism;
- an i-pair (G_t, L_c) has been transformed uniquely into a hypergraph HG_t;
- for computational purposes, some auxiliary constructions have been introduced—incidence matrix $\mathscr{F}(G_t)$ and multigraph MG_t; both maintain the isomorphism of dynamical systems.

The advantages of hypergraph representation compared with a more simple i-pair representation given in Section 2 are the following: (1) no additional parameter to distinguish non-isomorphic dynamical systems are needed; (2) a standard graph isomorphism algorithm can be used to establish the isomorphism of multigraphs; (3) the size of constructed multigraphs is approximately one half of that for G_t. Some results of MATHEMATICA implementation of this procedure are given in the next section.

5. MATHEMATICA implementation

Details of our MATHEMATICA implementation can be found in Ref. [20] (solutions of (1) and geometrical structure) and in Ref. [21] (topological structure and dynamical systems). General computation schema is the following. We implemented an algorithm sketched in Section 2, computed all solutions of (1) and used the MATHEMATICA package ‘‘DiscreteMath ‘Combinatorica’ ’’ to plot the triangle graph G_t, and to construct the incidence matrix $\mathfrak{F}$ and the multigraph MG_t. To establish multigraph isomorphism we

modified a standard algorithm provided by the "DiscreteMath 'Combinatorica' " package, because it can only be used for simple graphs and multigraphs with unlabeled edges. Some necessary conditions of multigraph isomorphism are checked as a preliminary step, in order to make computations faster. As output, the list of all resulting clusters is given, for each of them the corresponding incidence matrices, hypergraphs, and dynamical systems are written out (in the real form, to spare the place), and graphs G_t and MG_t are plotted. We also compute how many isomorphic clusters of each form appear in the chosen computation domain. Results for computation domain $D = 50$ are given below.

1. 18 systems: $(V_{HG} = \{1\}, E_{HG} = \{\{1\}, \{1\}, \{1\}\})$

$$\begin{pmatrix} 1 \\ 1 \\ 1 \end{pmatrix} \quad \begin{aligned} \dot{A}_1 &= \alpha_1 A_2 A_3, \\ \dot{A}_2 &= \alpha_2 A_1 A_3, \\ \dot{A}_3 &= \alpha_3 A_1 A_2. \end{aligned}$$

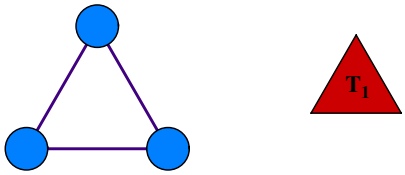

2. 4 systems: $(V_{HG} = \{1, 2\},\ E_{HG} = \{\{1\}, \{1\}, \{2\}, \{2\}, \{1, 2\}\})$

$$\begin{pmatrix} 1 & 0 \\ 1 & 0 \\ 0 & 1 \\ 0 & 1 \\ 1 & 1 \end{pmatrix} \quad \begin{aligned} \dot{A}_1 &= \alpha_1 A_2 A_5, \\ \dot{A}_2 &= \alpha_2 A_1 A_5, \\ \dot{A}_3 &= \alpha_4 A_4 A_5, \\ \dot{A}_4 &= \alpha_5 A_3 A_5, \\ \dot{A}_5 &= \tfrac{1}{2}(\alpha_3 A_1 A_2 + \alpha_6 A_3 A_4). \end{aligned}$$

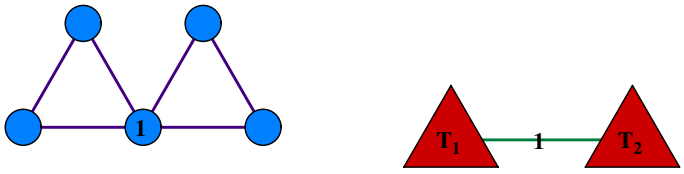

3. 1 system: $(V_{HG} = \{1, 2, 3\}, E_{HG} = \{\{1\}, \{1\}, \{2\}, \{3\}, \{3\}, \{1, 2\}, \{2, 3\}\})$

$$\begin{pmatrix} 1 & 0 & 0 \\ 1 & 0 & 0 \\ 0 & 1 & 0 \\ 0 & 0 & 1 \\ 0 & 0 & 1 \\ 1 & 1 & 0 \\ 0 & 1 & 1 \end{pmatrix} \quad \begin{aligned} \dot{A}_1 &= \alpha_1 A_2 A_6, \\ \dot{A}_2 &= \alpha_2 A_1 A_6, \\ \dot{A}_3 &= \alpha_4 A_6 A_7, \\ \dot{A}_4 &= \alpha_7 A_5 A_7, \\ \dot{A}_5 &= \alpha_8 A_4 A_7, \\ \dot{A}_6 &= \tfrac{1}{2}(\alpha_3 A_1 A_2 + \alpha_5 A_3 A_7), \\ \dot{A}_7 &= \tfrac{1}{2}(\alpha_9 A_4 A_5 + \alpha_6 A_3 A_6). \end{aligned}$$

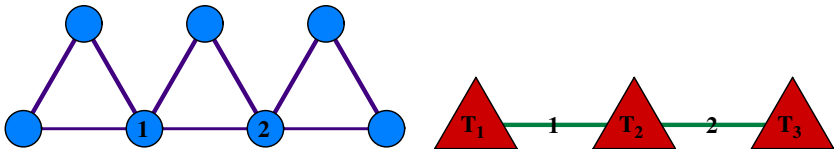

4. 2 systems: $(V_{HG} = \{1,2,3,4\}, E_{HG} = \{\{1\},\{1\},\{2\},\{2\},\{3\},\{4\},\{4\},\{3,4\},\{1,2,3\}\})$

$$\begin{pmatrix} 1 & 0 & 0 & 0 \\ 1 & 0 & 0 & 0 \\ 0 & 1 & 0 & 0 \\ 0 & 1 & 0 & 0 \\ 0 & 0 & 1 & 0 \\ 0 & 0 & 0 & 1 \\ 0 & 0 & 0 & 1 \\ 0 & 0 & 1 & 1 \\ 1 & 1 & 1 & 0 \end{pmatrix}$$

$$\begin{aligned} \dot{A}_1 &= \alpha_1 A_2 A_9, \\ \dot{A}_2 &= \alpha_2 A_1 A_9, \\ \dot{A}_3 &= \alpha_4 A_4 A_9, \\ \dot{A}_4 &= \alpha_5 A_3 A_9, \\ \dot{A}_5 &= \alpha_7 A_8 A_9, \\ \dot{A}_6 &= \alpha_{10} A_7 A_8, \\ \dot{A}_7 &= \alpha_{11} A_6 A_8, \\ \dot{A}_8 &= \tfrac{1}{2}(\alpha_{12} A_6 A_7 + \alpha_8 A_5 A_9), \\ \dot{A}_9 &= \tfrac{1}{3}(\alpha_3 A_1 A_2 + \alpha_6 A_3 A_4 + \alpha_9 A_5 A_8), \end{aligned}$$

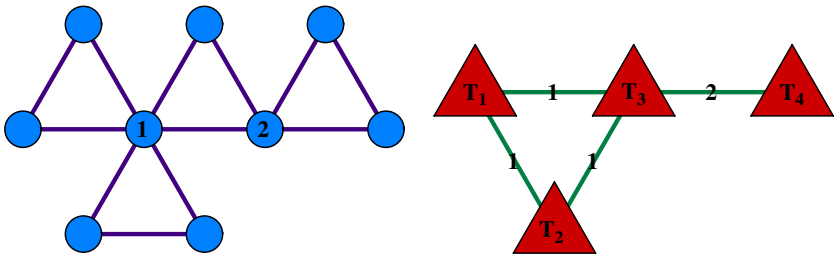

5. 1 system: $(V_{HG} = \{1,2,3,4\}, E_{HG} = \{\{1\},\{1\},\{2\},\{3\},\{4\},\{4\},\{1,2\},\{2,3\},\{3,4\}\})$

$$\begin{pmatrix} 1 & 0 & 0 & 0 \\ 1 & 0 & 0 & 0 \\ 0 & 1 & 0 & 0 \\ 0 & 0 & 1 & 0 \\ 0 & 0 & 0 & 1 \\ 0 & 0 & 0 & 1 \\ 1 & 1 & 0 & 0 \\ 0 & 1 & 1 & 0 \\ 0 & 0 & 1 & 1 \end{pmatrix}$$

$$\begin{aligned} \dot{A}_1 &= \alpha_1 A_2 A_7, \\ \dot{A}_2 &= \alpha_2 A_1 A_7, \\ \dot{A}_3 &= \alpha_4 A_7 A_8, \\ \dot{A}_4 &= \alpha_7 A_8 A_9, \\ \dot{A}_5 &= \alpha_{10} A_6 A_9, \\ \dot{A}_6 &= \alpha_{11} A_5 A_9, \\ \dot{A}_7 &= \tfrac{1}{2}(\alpha_3 A_1 A_2 + \alpha_5 A_3 A_8), \\ \dot{A}_8 &= \tfrac{1}{2}(\alpha_6 A_3 A_7 + \alpha_8 A_4 A_9), \\ \dot{A}_9 &= \tfrac{1}{2}(\alpha_{12} A_5 A_6 + \alpha_9 A_4 A_8). \end{aligned}$$

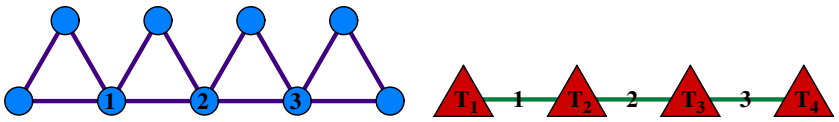

6. 1 system: $(V_{HG} = \{1,2,3,4,5\}, E_{HG} = \{\{1\},\{1\},\{2,4\},\{2,5\},\{3,4\},\{3,5\},\{4,5\},\{1,2,3\}\})$

$$\begin{pmatrix} 1 & 0 & 0 & 0 & 0 \\ 1 & 0 & 0 & 0 & 0 \\ 0 & 1 & 0 & 1 & 0 \\ 0 & 1 & 0 & 0 & 1 \\ 0 & 0 & 1 & 1 & 0 \\ 0 & 0 & 1 & 0 & 1 \\ 0 & 0 & 0 & 1 & 1 \\ 1 & 1 & 1 & 0 & 0 \end{pmatrix}$$

$$\begin{aligned} \dot{A}_1 &= \alpha_1 A_2 A_8, \\ \dot{A}_2 &= \alpha_2 A_1 A_8, \\ \dot{A}_3 &= \tfrac{1}{2}(\alpha_{10} A_5 A_7 + \alpha_4 A_4 A_8), \\ \dot{A}_4 &= \tfrac{1}{2}(\alpha_{13} A_6 A_7 + \alpha_5 A_3 A_8), \\ \dot{A}_5 &= \tfrac{1}{2}(\alpha_{11} A_3 A_7 + \alpha_7 A_6 A_8), \\ \dot{A}_6 &= \tfrac{1}{2}(\alpha_{14} A_4 A_7 + \alpha_8 A_5 A_8), \\ \dot{A}_7 &= \tfrac{1}{2}(\alpha_{12} A_3 A_5 + \alpha_{15} A_4 A_6), \\ \dot{A}_8 &= \tfrac{1}{3}(\alpha_3 A_1 A_2 + \alpha_6 A_3 A_4 + \alpha_9 A_5 A_6). \end{aligned}$$

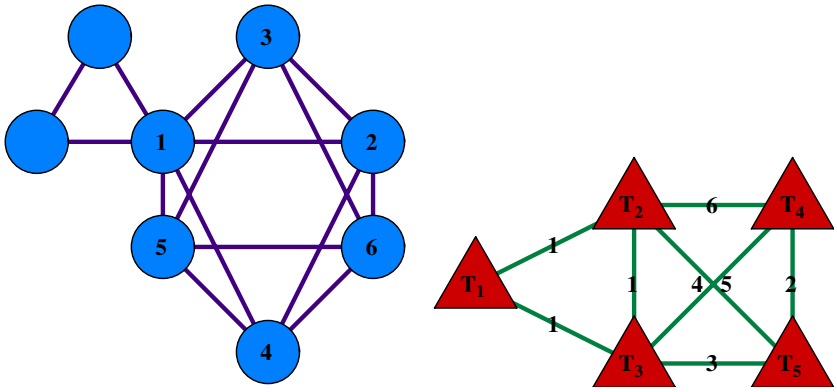

7. 1 system: $(V_{HG}\{1,2,3,4,5,6,7\}, E_{HG} = \{\{2\},\{3\},\{4\},\{7\},\{7\},\{1,2\},\{1,3\},\{2,6\},\{4,5\},\{5,6\},\{6,7\},\{1,3,4,5\}\})$

$$\begin{pmatrix} 0 & 1 & 0 & 0 & 0 & 0 & 0 \\ 0 & 0 & 1 & 0 & 0 & 0 & 0 \\ 0 & 0 & 0 & 1 & 0 & 0 & 0 \\ 0 & 0 & 0 & 0 & 0 & 0 & 1 \\ 0 & 0 & 0 & 0 & 0 & 0 & 1 \\ 1 & 1 & 0 & 0 & 0 & 0 & 0 \\ 1 & 0 & 1 & 0 & 0 & 0 & 0 \\ 0 & 1 & 0 & 0 & 0 & 1 & 0 \\ 0 & 0 & 0 & 1 & 1 & 0 & 0 \\ 0 & 0 & 0 & 0 & 1 & 1 & 0 \\ 0 & 0 & 0 & 0 & 0 & 1 & 1 \\ 1 & 0 & 1 & 1 & 1 & 0 & 0 \end{pmatrix}$$

$$\begin{aligned}
\dot{A}_1 &= \alpha_4 A_6 A_8, \\
\dot{A}_2 &= \alpha_7 A_7 A_{12}, \\
\dot{A}_3 &= \alpha_{10} A_9 A_{12}, \\
\dot{A}_4 &= \alpha_{19} A_5 A_{11}, \\
\dot{A}_5 &= \alpha_{20} A_4 A_{11}, \\
\dot{A}_6 &= \tfrac{1}{2}(\alpha_5 A_1 A_8 + \alpha_1 A_7 A_{12}), \\
\dot{A}_7 &= \tfrac{1}{2}(\alpha_8 A_2 A_{12} + \alpha_2 A_6 A_{12}), \\
\dot{A}_8 &= \tfrac{1}{2}(\alpha_6 A_1 A_6 + \alpha_{16} A_{10} A_{11}), \\
\dot{A}_9 &= \tfrac{1}{2}(\alpha_{11} A_3 A_{12} + \alpha_{13} A_{10} A_{12}), \\
\dot{A}_{10} &= \tfrac{1}{2}(\alpha_{17} A_8 A_{11} + \alpha_{14} A_9 A_{12}), \\
\dot{A}_{11} &= \tfrac{1}{2}(\alpha_{21} A_4 A_5 + \alpha_{18} A_8 A_{10}), \\
\dot{A}_{12} &= \tfrac{1}{4}(\alpha_9 A_2 A_7 + \alpha_3 A_6 A_7 + \alpha_{12} A_3 A_9 + \alpha_{15} A_9 A_{10}).
\end{aligned}$$

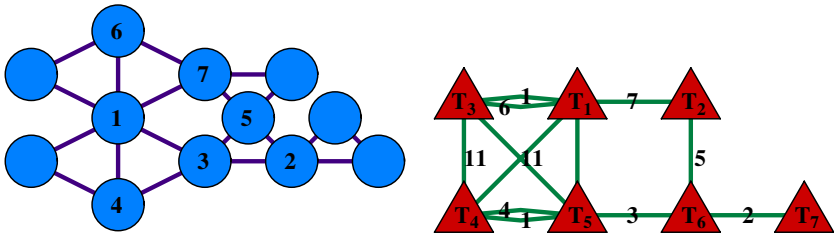

These results show that in the spectral domain $|\vec{k}| \leqslant 50$ which contains $\sim 2 \times 10^3$ Fourier harmonics we have only seven non-isomorphic dynamical systems (clusters of waves) for further analytical and numerical study. Some of them, for instance (6), are known to be solved explicitly in Jacobean elliptic functions (example of explicit expressions for the case of spherical planetary waves can be found in Ref. [22]). Knowledge of the explicit form of a dynamical system allows sometimes to obtain a few conservation laws as in the case (7) and simplify substantially further numerical investigations of these systems. It is important to understand that though *qualitative* properties of all isomorphic clusters are the same, their *quantitative* properties depend on the magnitudes of coupling coefficients α_i, of course. Computation of these coefficients is usually done by standard multi-scale method which is tedious but completely algorithmic procedure and can also be programmed in MATHEMATICA (see Ref. [20] for its implementation).

6. Two mechanisms to destroy clusters

There are two mechanisms which can destroy clusters constructed above: (1) increasing of the spectral domain D, and (2) taking into account quasi-resonances, i.e. integer solutions of

$$\omega_1 \pm \omega_2 \pm \cdots \pm \omega_s = \Omega > 0, \quad \vec{k}_1 \pm \vec{k}_2 \pm \cdots \pm \vec{k}_s = 0 \tag{17}$$

with some non-zero resonance width Ω. Below we regard briefly both of them.

6.1. Increasing of spectral domain

Obviously, the structure of clusters becomes simpler with diminishing of the domain D—some solutions (triads) disappear. On the other hand, increasing of D might lead to substantial changes of the structure. Thus it is important to understand how solution structure depends on the chosen computation domain. With this aim let us re-write first equation of (3) in the form

$$\frac{1}{k_1} + \frac{1}{k_2} = \frac{1}{k_3} \tag{18}$$

and notice that $k_3 < k_1$ and $k_3 < k_2$. Introducing notations k_-, k_0, k_+ for the minimal, intermediate and maximal of the numbers k_1, k_2, k_3 we see that $k_3 = k_-$. This yields

$$\frac{1}{k_-} = \frac{1}{k_+} + \frac{1}{k_0} \leqslant \frac{2}{k_0} \Rightarrow k_0 \leqslant 2k_- \quad \text{and} \quad k_+ = \frac{k_0 k_-}{k_0 - k_-} \leqslant 2k_-^2.$$

We conclude that wave interactions are *local* in the following sense: the lengths of wave vectors constructing a solution of (3) cannot be too far apart. In particular, if we are interested in the solution structure in the domain, say, $k_i \leqslant D = 50$, it is enough to investigate a larger domain $\widetilde{D} = 2 \times 50^2 = 5000$, in order to establish which clusters stay unchanged and to find those which are enhanced via solutions with wave vectors lying outside of the initial domain $D = 50$.

6.2. Quasi-resonances

It was shown in Ref. [24] that for discrete quasi-resonances to be able to start some *low boundary* for resonance width Ω can be written out explicitly. It is interesting that for many dispersion functions there exist a *global* low boundary for most clusters which does not depend on the spectral domain under consideration and also does not depend on the number of interacting waves s. For instance, in case of $\omega = (m^2 + n^2)^{1/4}$ (gravity water waves) the use of the generalized Thue–Siegel–Roth theorem [25] yields $\Omega > 1$. Obviously, for an arbitrary dispersion function a *local* low boundary exists which is defined by the spectral domain $T = \{(m,n) : 0 < |m|, |n| \leqslant D < \infty\}$ chosen for numerical simulations. Indeed, let us define $\Omega_D = \min_p \Omega_p$, where

$$\Omega_p = |\omega(\vec{k}_1^p) \pm \omega(\vec{k}_2^p) \pm \cdots \pm \omega(\vec{k}_s^p)|, \quad \vec{k}_j^p = (m_j^p, n_j^p) \in T, \quad \forall j = 1, 2, \ldots, s,$$

and

$$\omega(\vec{k}_1^p) \pm \omega(\vec{k}_2^p) \pm \cdots \pm \omega(\vec{k}_s^p) \neq 0 \quad \forall p,$$

and index p runs over all wave vectors in T, i.e. $p \leqslant 4D^2$. Obviously, the so defined Ω_p is a non-zero number as the minimum of a finite number of non-zero numbers and Ω_D is minimal resonance width which allows discrete quasi-resonances to start, for chosen D.

Physically important resonance width Ω_{phys} is defined by the accuracy of computations and precision of measurements in numerical and laboratory experiments correspondingly. Quasi-resonances with $\Omega_D > \Omega_{phys}$ will not destroy the clusters.

7. Discussion

In order to apply the theory of discrete resonances to a real physical problem, a profound study of constructed dynamical systems is needed. It is well-known that dynamical system (6) demonstrates periodic energy exchange between the modes of a triad. On the other hand, dynamical systems consisting of a few connected triads have enough degrees of freedom $\mathcal{N}$ to behave chaotically. The question of major importance therefore is to discern between two classes of situations: (1) resonance clusters with periodic energy exchange within each cluster, and (2) those which can be described statistically, similar to the kinetic equation approach. From this point of view, all our theoretical results and symbolical programming can be regarded as an introductory step for further numerical simulations.

We are quite aware of the fact that there exist a multitude number of important questions to be answered in order to understand a very complicated mutual relationship between discrete and statistical regimes of wave system dynamics. For instance, is the corresponding statistical dynamics close to Gaussian? Is the probability of attractor appearance in the subspace generated by integrals of motion uniformly distributed? What is the minimal value of $\mathcal{N}$ allowing to "forget" topological details of the discrete, low-dimensional dynamical system and describe the corresponding dynamical system statistically? How does energy exchange between isolated and continuous subsystems look like? What is the role of nonlinearity in triggering energy flux toward small scales? Is it possible to develop some analytical tools for description of low-dimensional systems (for example, a generalized kinetic equation that accounts for the finite width of frequency resonances)? etc.

A first feeling of possible answers to some of these questions can be obtained by computer simulations with a few well-chosen dynamical systems with degrees of freedom from $\mathcal{N} = 4$ to $10 \div 20$ which is on our agenda. Notice that in the case of 3-wave resonances one has to construct dynamical systems as it was done above and choose those which are not enhanced by increasing the computation domain. Choice of initial conditions for numerical simulations would be another important subject to study for, as it was mentioned in Ref. [22], even for one isolated resonant triad it is always possible to choose initial energy distribution among the modes in such a way that the period of their energy exchange will tend to infinity.

In general, our graph-theoretical approach can be used, with appropriate refinements, also for s-wave resonances, with $s \geqslant 4$. In this last case, existence of different types of resonances, spectrum anisotropy, etc. [24] have also to be taken into account in order to choose representative dynamical systems for numerical simulations.

The same approach (algorithms from [16], graph construction, etc.) can also be used directly for any mesoscopic system with resonances of a more general form

$$p_1\omega_1 \pm p_2\omega_2 \pm \cdots \pm p_s\omega_s = 0, \quad p_1\vec{k}_1 \pm p_2\vec{k}_2 \pm \cdots \pm p_s\vec{k}_s = 0 \tag{19}$$

with integer p_i.

Acknowledgments

Authors acknowledge the support of the Austrian Science Foundation (FWF) under projects SFB F013/F1304 and SFB F013/F1301. Authors are very grateful to anonymous referees for their valuable remarks, suggestions and improvements.

References

[1] P. Denissenko, S. Lukaschuk, S. Nazarenko, E-print: arXiv.org:nlin.CD/0610015, 2006.
[2] R. Toral, C.J. Tessone, Commun. Comput. Phys. 2 (2) (2007) 177–195.
[3] A. Stefanovska, M.B. Lotric, S. Strle, H. Haken, Physiol. Meas. 22 (2001) 535–550.
[4] H. Spohn, E-print arXiv:math-ph/0605069, 2006.
[5] E.A. Kartashova, Phys. Rev. Lett. 72 (1994) 2013–2016.
[6] V.E. Zakharov, V.S. L'vov, G. Falkovich, Kolmogorov Spectra of Turbulence, Series in Nonlinear Dynamics, Springer, Berlin, 1992.
[7] E.A. Kartashova, AMS Transl. 2 (1998) 95–129.
[8] C. Connaughton, S. Nazarenko, A. Pushkarev, Phys. Rev. E 63 (4) (2001) 046306.
[9] Yu.V. Lvov, S. Nazarenko, B. Pokorni, Physica D 218 (2006) 24–35.

[10] M. Tanaka, J. Fluid Mech. 444 (2001) 199–221.
[11] M. Tanaka, Fluid Dyn. Res. 82 (1) (2001) 41–60.
[12] M. Tanaka, N. Yokoyama, Fluid Dyn. Res. 34 (3) (2004) 199–216.
[13] M. Tanaka, J. Phys. Oceanogr. 77 (2007) 1022–1036.
[14] V.E. Zakharov, A.O. Korotkevich, A.N. Pushkarev, A.I. Dyachenko, JETP Lett. 82 (8) (2005) 487–491.
[15] E. Kartashova, JETP Lett. 83 (7) (2006) 341–345.
[16] E. Kartashova, J. Low Temp. Phys. 145 (1–4) (2006) 286–295;
E. Kartashova, A. Kartashov, Int. J. Mod. Phys. C 17 (11) (2006) 1579–1596;
E. Kartashova, A. Kartashov, Commun. Comput. Phys. 2 (4) (2007) 783–794;
E. Kartashova, A. Kartashov, Physics A 380 (2007) 66–74.
[17] J. Pedlosky, Geophysical Fluid Dynamics, second ed., Springer, Berlin, 1987.
[18] E.A. Kartashova, G.M. Reznik, Oceanology 31 (1992) 385–389.
[19] J.M. Basilla, Proc. Jpn. Acad. 80 (Ser. A) (2004) 40.
[20] Ch. Feurer, E. Kartashova, G. Mayrhofer, C. Raab, W. Schreiner, RISC Report Series, May, 2007.
[21] E. Kartashova, G. Mayrhofer, RISC Report Series, May, 2007.
[22] E. Kartashova, V.S. L'vov, Phys. Rev. Lett. 98 (19) (2007) 198501.
[24] E. Kartashova, Phys. Rev. Lett. May 98 (21) (2007) 214502.
[25] W.M. Schmidt, Diophantine approximations, Mathematical Lecture Notes, vol. 785, Springer, Berlin, 1980.